Effect of Turbulence Fluctuations on Surface Heating Rate in Hypersonic Turbulent Boundary Layers

Lian Duan* and M. Pino Martín†

Princeton University, Princeton, NJ, 08544

In this paper, we investigate the effect of turbulence fluctuations on surface heating rate by conducting direct numerical simulations (DNS) of reacting hypersonic turbulent boundary layers at conditions typical of reentry vehicles. Surface heat fluxes, including conductive heat flux and catalytic heat flux, are computed and compared for both supercatalytic and noncatalytic walls. At all conditions considered, it is found that turbulence fluctuations cause large fluctuations in surface heat flux. The instantaneous heat load on the surface can be as large as about 1.7 times the mean value for the condition considered. Turbulence fluctuations have subtle influence on the mean heating rate. We also find that the effect of turbulence-chemistry interaction on surface heating rate is insignificant at all conditions considered.

Nomenclature

t	time
x	streamwise coordinate
y	spanwise coordinate
z	wall-normal coordinate
$\hat{R}$	universal gas constant, 8.314, J/(mole·K)
κ	mixture thermal conductivity, J/(K·m·s)
μ	mixture viscosity, kg/(m·s)

*Ph.D. Student, Department of Mechanical and Aerospace Engineering. AIAA Student Member.
†Assistant Professor, Department of Mechanical and Aerospace Engineering, AIAA Senior Member.

ρ density, kg/m^3

σ_{ij} shear stress tensor, $\sigma_{ij} = 2\mu S_{ij} - \frac{2}{3}\mu\delta_{ij}S_{kk}$, Pa

c_p specific heat at constant pressure, J/(kg·K)

c_v specific heat at constant volume, J/(kg·K)

D mixture mass diffusivity, m^2/s

E total energy, J/m^3

h specific enthalpy, J/kg

h° heat of formation, J/kg

k_b backward reaction coefficient

k_f forward reaction coefficient

K_{eq} equilibrium constant

M molecular weight, kg/mole

p pressure, $p = \sum_s \rho_s \frac{\hat{R}}{M_s} T$, Pa

Pr Prandtl number, $Pr = \frac{\mu Cp}{\kappa}$

q heat flux, $q_j = -\kappa \frac{\partial T}{\partial x_j}$, J/(m^2·s)

S_{ij} strain rate tensor, $S_{ij} = \frac{1}{2}(\partial u_i/\partial x_j + \partial u_j/\partial x_i)$, s^{-1}

T translational temperature, K

u mass-averaged velocity, m/s

v diffusion velocity, m/s

w production rate, kg/(m^3·s)

Subscripts

δ boundary layer edge quantity

a, m atom, molecule

i, j Cartesian coordinate directions or species

n wall normal direction

s species variable

w wall quantity

I. Introduction

One of the most important tasks in designing hypersonic vehicles is to predict aerothermodynamic heating. When the boundary layer on hypersonic vehicles is turbulent, fluctuations appear in the temperature and species composition, which in turn introduce fluctuations in the surface heating rate. Although the mean heating rate can be predicted fairly accurately by some widely used engineering codes [1], the fluctuations in surface heat flux are still largely uncertain.

Another factor that is typically neglected in hypersonic vehicle design is the turbulence-chemistry interaction. For a turbulence flow, fluctuations in the species production rate $w_s(T, \rho_s)$ are caused by fluctuations in temperature and species composition. Because of the nonlinear dependence of w_s on its parameters, we have

$$\overline{w}_s(T, \rho_s) \neq w_s(\overline{T}, \overline{\rho}_s)$$

and the difference is due to the turbulence-chemistry interaction. Although turbulence-chemistry interaction is studied extensively in the field of combustion, [2–8], and has been found extremely important for predicting combustion quantities, such as burning rates and ignition delay, its influence on surface heating rate for hypersonic applications is still largely unknown.

In this paper, we consider two configurations under typical hypersonic conditions to estimate the magnitude of the fluctuating heating rates and assess errors in predicting surface heat flux when neglecting the chemistry-turbulence interaction. In particular, we consider a slender body resembling the configuration and flow conditions of the Reentry F experiment [1] , and a blunt body configuration.

The paper is structured as follows. The governing equations and numerical methods for DNS are given in Sections II and III, respectively; the surface heat flux calculation and surface catalytic boundary conditions are introduced in Section IV; Flow conditions are given in Section V; Results are presented in Section VI. Finally, conclusions are drawn in Section VII.

II. Governing Equations

The equations describing the unsteady motion of a reacting fluid are given by the species mass, mass-averaged momentum, and total energy conservation equations, which, neglecting thermal non-equilibrium, are

$$\begin{aligned}
\frac{\partial \rho_s}{\partial t} + \frac{\partial}{\partial x_j}\Big(\rho_s u_j + \rho_s v_{sj}\Big) &= w_s \\
\frac{\partial \rho u_i}{\partial t} + \frac{\partial}{\partial x_j}\Big(\rho u_i u_j + p\delta_{ij} - \sigma_{ij}\Big) &= 0 \\
\frac{\partial E}{\partial t} + \frac{\partial}{\partial x_j}\Big((E+p)u_j - u_i\sigma_{ij} + q_j + \sum_s \rho_s v_{sj} h_s\Big) &= 0
\end{aligned} \tag{1}$$

The total energy E is given by

$$E = \sum_s \rho_s c_{vs} T + \frac{1}{2}\rho u_i u_i + \sum_s \rho_s h_s^\circ, \tag{2}$$

In general, w_s is a function of temperature and species composition, i.e. $w_s = w_s(T, \rho_s)$. To derive the explicit expression for w_s, consider a reaction where species $S1$ reacts to form species $S2$

$$S1 + M \rightleftharpoons S2 + M \tag{3}$$

where M is a collision partner, which is either $S1$ or $S2$ in this case. The source terms for $S1$ and $S2$ can be written using law of mass action

$$w_{S1} = -M_{S1} k_f \frac{\rho_{S1}}{M_{S1}} \left(\frac{\rho_{S1}}{M_{S1}} + \frac{\rho_{S2}}{M_{S2}} \right) + M_{S1} k_b \frac{\rho_{S2}}{M_{S2}} \left(\frac{\rho_{S1}}{M_{S1}} + \frac{\rho_{S2}}{M_{S2}} \right) = w_f + w_b \tag{4}$$

and $w_{S2} = -w_{S1}$; k_f and k_b are forward and backward reaction rates respectively. These are written as

$$k_f = C_f T^\eta e^{-\theta/T}, \qquad k_b = \frac{k_f}{K_{eq}}, \tag{5}$$

where K_{eq} is the temperature-dependent equilibrium constant.

For a two species mixture, the diffusive mass flux can be accurately represented using Fick's law

$$j_s = \rho_s v_{sj} = -\rho D \frac{\partial c_s}{\partial x_j}, \tag{6}$$

and D is given in terms of the Lewis number

$$Le = \frac{\rho D Pr}{\mu}, \tag{7}$$

μ and κ are calculated by Gupta [9]-Yos [10] mixing rule, and Le is taken to be unity, so that the energy transport due to mass diffusion is equal to the energy transport due to thermal conduction.

III. Numerical Methods

The spatial derivatives are computed using a fourth-order accurate WENO scheme [11]. The WENO scheme prevents oscillations near shock waves without introducing excessive dissipation and offer very high resolution in smooth regions. Since the Riemann problem resulting from WENO reconstruction is computationally expensive to solve exactly, an approximate Riemann solver is used. One of the most commonly used approximate Riemann solvers is Roe scheme, which was derived by Roe [12] for perfect gas. For chemically reacting flows,

the Roe scheme needs to be generalized to include multicomponent and non-equilibrium effects [13].

To perform the numerical integration, we use a third-order accurate low-storage Runge-Kutta method by Williamson [14]. The viscous terms are computed using a fourth-order accurate central scheme. An extensive description of code validation is given in Duan & Martin. [15]

IV. Heat Transfer and Catalysis

In a chemically reacting flow, the heat transfer to a surface is composed of the usual conduction term plus an additional term, which results from diffusion of species to the surface and depends on the catalytic property of the surface. We can write this as

$$q_{total} = q_{cond} + q_{cata} = \kappa \frac{\partial T}{\partial z} + \sum_{s=1}^{ns} \beta_\beta h_s^\circ j_s \tag{8}$$

where β_i is the chemical energy accommodation coefficient, which is the ratio of chemical energy transferred to the surface compared to the available energy from recombination and is taken to be unity in the current simulations; and j_s is the normal diffusive mass flux given by Fick's law.

In the case of a noncatalytic wall in a binary mixture, the species concentration gradient is zero at the wall.

$$\frac{\partial c_a}{\partial z} = -\frac{\partial c_m}{\partial z} = 0 \tag{9}$$

Another limiting case is a supercatalytic wall, which assumes that all the atoms at the surface recombine. The corresponding boundary condition for atomic species becomes

$$c_a = 0$$

V. Flow conditions

We evaluate the influence of turbulence fluctuations on the surface heating rate under two typical hypersonic conditions, which are denoted by Angle32 and Angle05. These cases represent the boundary layer on configurations with half cone angle of 32°, typical of a blunt body reentry vehicle, and 5°, similar to the Reentry F experiment. Both configurations are assumed to fly at $80,000$ ft with a Mach number of 21. The boundary layer edge conditions and wall parameters are given in table 1, which provides edge Mach number, density, and temperature, M_δ, ρ_δ and T_δ, respectively, and boundary property: momentum thickness, θ, shape factor, $H = \delta^*/\theta$, where δ^* is the displacement thickness, boundary layer thickness

δ, and different definitions of Reynolds number, where $Re_\theta \equiv \frac{\rho_\delta u_\delta \theta}{\mu_\delta}$, $Re_\tau \equiv \frac{\rho_w u_\tau \delta}{\mu_w}$, and $Re_{\delta 2} \equiv \frac{\rho_\delta u_\delta \theta}{\mu_w}$.

Case	M_δ	ρ_δ(kg/m^3)	T_δ(K)	T_w(K)	Re_θ	Re_τ	$Re_{\delta 2}$	θ(mm)	H	δ(mm)
Angle32	4.37	0.467	3326.1	2400	672.5	394.7	784.4	0.03	2.70	0.314
Angle05	14.1	0.115	656.4	3000	2886.8	388.8	1033.2	0.170	33.5	7.52

Table 1. Dimensional bounday layer edge and wall parameters for direct numerical simulations

Under these conditions, the dominant reactions in the air are the dissociation-recombination of oxygen, $O_2 + M \rightleftharpoons 2O + M$, which we use as reaction mechanism to simplify the analysis. For each case, both noncatalytic and supercatalytic walls are considered.

The flow field is initialized following the procedure given by Martin [16]. The domain size is about $8\delta \times 2\delta \times 15\delta$ in stream-wise, span-wise, and wall normal directions. The number of grid points is $440 \times 240 \times 125$. Periodic boundary conditions are used in stream-wise and span-wise directions.

Since the initial state is not physical, there is an initial transient of flow field to physical state. Figure 1 shows the temporal evolution of the friction velocity u_τ for Angle32 with supercatalytic wall condition. Around $\tau_t = 0.2$, where τ_t is non-dimensional time unit defined as $\tau_t = tu_\tau/\delta$, u_τ levels off, indicating the onset of equilibrium turbulence in the near-wall region. For the same case, Figure 2 plots the correlation between velocity fluctuation in stream-wise direction and temperature fluctuation at $\tau_t = 0.2, 0.6, 1.0$, indicating equilibrium of turbulence across the boundary layer. We gather statistics from $\tau_t = 0.2$ for around 0.6 non-dimensional time unit, which corresponds to about $60\delta^*/u_\delta$. During this period, the change in (δ^*, u_τ, C_f) is less than 5% and the flow can be viewed as a good approximation of a static station of a boundary layer. [16, 17]. Figure 3 plots the van-Driest transformed velocity, and Figure 4 plots the Morkovin-scaled turbulence intensities, which resemble those of a non–reacting boundary layer. A similar approach for gathering statistics is followed by all the other cases, and similar results are found.

VI. Results and Discussions

For simplicity, we use notations Angle32sup, Angle32non, Angle05sup and Angle05non to denote simulations of Angle32 with supercatalytic wall and noncatalytic wall, Angle05 with supercatalytic and noncatalytic walls, respectively.

A. Surface heat flux

We calculate the mean and RMS of q_{cond}, q_{cata} and q_{total} for all cases. To measure the influence of turbulence fluctuations on the mean heat flux, we define the amplification factor as follows:

$$\eta_q \equiv \frac{\overline{q(T,\rho_s)}}{q(\overline{T},\overline{\rho}_s)}$$

We will refer to the numerator as the 'turbulent' heat flux and the denominator as the 'laminar' heat flux. The 'laminar' heat flux is the heat flux we would compute if there were no turbulence fluctuations in temperature and species composition. If the ratio is close to one, the turbulence fluctuations do not contribute significantly to the mean heat flux.

Table 2 provides mean values, RMSs and amplification factors of q_{cond}, q_{cata} and q_{total} for all cases. It is shown that for all the cases, turbulence fluctuations cause large fluctuations in heat flux. For the case Angle05non, the magnitude of the fluctuation in total heat flux is as large as 73% of the mean value.

However, for all cases, the amplification factors for q_{cond}, q_{cata} and q_{total} are close to unity, indicating that fluctuations in temperature and species composition have nearly no influence on the mean surface heating rates. This is not unexpected. Since the thermal conductivity and the mass diffusivity are weak functions in T and ρ_s and can be considered nearly constant, Equation 8 shows that q_{cond}, q_{cata} and q_{total} are linear functions in T and ρ_s. As a result, $\overline{q(T,\rho_s)} \approx q(\overline{T},\overline{\rho}_s)$. This is quite different for the case for species production rate w_s, which has highly nonlinear dependence on the flow parameters, primarily on the temperature.

Case	$\overline{q}_{cond}$	$\overline{q}_{cata}$	$\overline{q}_{total}$	$(q'_{rms}/\overline{q})_{cond}$	$(q'_{rms}/\overline{q})_{cata}$	$(q'_{rms}/\overline{q})_{total}$	$\eta_{q_{cond}}$	$\eta_{q_{cata}}$	$\eta_{q_{total}}$
Angle32sup	3.16e7	1.27e7	4.43e7	0.56	0.36	0.49	1.00	1.00	1.00
Angle32non	3.22e7	0.00	3.22e7	0.52	0.0	0.52	1.00	1.00	1.00
Angle05sup	2.05e6	0.73e6	2.78e6	0.81	0.35	0.68	1.00	1.00	1.00
Angle05non	1.81e6	0.00	1.81e6	0.73	0.00	0.73	1.00	1.00	1.00

Table 2. Mean values, RMSs and amplification factors of q_{cond}, q_{cata} and q_{total}. The unit of $\overline{q}_{cond}$, $\overline{q}_{cata}$ and $\overline{q}_{total}$ is W/m^2.

B. Turbulence-chemistry interaction

We investigate the effect of turbulence-chemistry interaction on surface heat rating by doing simulations at the same freestream and wall conditions as cases in Table 2, except modeling

w_s using $w_s = w_s(\bar{T}, \bar{\rho}_s)$ for each case, where $\bar{T}$ and $\bar{\rho}_s$ are mean temperature and species density, respectively. By modeling w_s in this way, we neglect the influence of temperature and species composition fluctuations on production rate and as a result neglect the effect of turbulence-chemistry interaction. Heat fluxes are then calculated and compared with those including turbulence-chemistry interaction. Table 3 shows the relative difference in heat fluxes with and without considering turbulence-chemistry interaction for all cases. In the table, we denote the mean and RMS of heat fluxes without considering turbulence-chemistry interaction as $\tilde{q}$ and q''_{rms}, respectively. It is shown that turbulence-chemistry interaction has very subtle influence on the mean and RMS of heat fluxes for all cases, with maximum difference around 7%.

Case	$\lvert\frac{\tilde{q}-\overline{q}}{\overline{q}}\rvert_{cond}$	$\lvert\frac{\tilde{q}-\overline{q}}{\overline{q}}\rvert_{cata}$	$\lvert\frac{\tilde{q}-\overline{q}}{\overline{q}}\rvert_{total}$	$\lvert\frac{q''_{rms}-q'_{rms}}{q'_{rms}}\rvert_{cond}$	$\lvert\frac{q''_{rms}-q'_{rms}}{q'_{rms}}\rvert_{cata}$	$\lvert\frac{q''_{rms}-q'_{rms}}{q'_{rms}}\rvert_{total}$
Angle32sup	0.30%	0.32%	0.12%	0.53%	1.62%	0.64%
Angle32non	0.32%	0.00%	0.32%	3.64%	0.00%	3.64%
Angle05sup	2.52%	4.13%	0.76%	2.70%	6.84%	3.40%
Angle05non	2.12%	0.00%	2.12%	2.87%	0.00%	2.87%

Table 3. Relative difference in mean and RMS of q_{cond}, q_{cata} and q_{total} with and without including turbulence-chemistry interaction.

VII. Conclusions

We conduct DNS of turbulence boundary layers at typical hypersonic conditions to investigate the influence of turbulence fluctuations as well as turbulence-chemistry interaction on surface heating rates. For the conditions considered, it is found that turbulence fluctuations cause large fluctuations in surface heat flux, while they have nearly no influence on the mean heat flux. It is also shown that the effect of turbulence-chemistry interaction has minor influence on surface heat flux. It should be noticed that the turbulence-chemistry interaction is weak for the chosen conditions.

VIII. Acknowledgment

This work is sponsored by the Air Force Office of Scientific Research under Grant FA9550-05-1-0490 and NASA under Grant NNX08AD04A. We would like to acknowledge Peter Gnoffo for his help in the selection and assessment of the flow conditions.

References

[1]R.A. Thompson, E.V. Zoby, K.E. Wurster, and P.A. Gnoffo. Aerothermodynamic study of slender conical vehicles. *J. Thermophysics*, 3(4):361–367, 1989.

[2]P.A. Libby and F.A. Williams. Turbulent reacting flows. *Academic Press, New York*, 1994.

[3]R.L. Gaffney, J.A. White, S.S. Girimaji, and J.P. Drummond. Modeling temperature and species fluctuations in turbulent reacting flow. *Computing Systems in Engineering*, 5(2):117–133, 1994.

[4]B.J. Delarue and S.B. Pope. Calculations of subsonic and supersonic turbulent reacting mixing layers using probability density function methods. *Physics of Fluids*, 10(2):487–498, 1998.

[5]A.T. Hsu, Y.-L.P. Tsai, and M.S. Raju. Probability density function approach for compressible turbulent reacting flows. *AIAA Journal*, 32(7):1407–1415, 1994.

[6]W.H. Calhoon and D.C. Kenzakowski. Assessment of turbulence-chemistry interactions in missile exhaust plume signature. *Journal of Spacecraft*, 40(5):694–695, 2003.

[7]R.A. Baurle and S.S. Girimaji. Assumed PDF turbulence-chemistry closure with temperature-composition correlations. *Combustion and Flames*, 134:131–148, 2003.

[8]P. Gerlinger, B. Noll, and M. Aigner. Assumed pdf modeling and pdf structure investigation using finite-rate chemistry. *Progress in computational fluid dynamics*, 5:334–344, 2005.

[9]R.N. Gupta, J.M. Yos, R.A. Thompson, and K.P. Lee. A review of reaction rates and thermodynamic and transport properties for 11-species air model for chemical and thermal nonequilibrium calculations to 30000K. *NASA RP-1232*, 1990.

[10]J.M. Yos. Transport properties of nitrogen, hydrogen, oxygen, and air to 30,000 k. *Avco. Corp. TR AD-TM-63-7*, 1963.

[11]E.M. Taylor, M. Wu, and M.P Martin. Optimization of nonlinear error sources for weighted non-oscillatory methods in direct numerical simulations of compressible turbulence. *Journal of Computational Physics*, 223:384–397, 2006.

[12]P.L.Roe. Approximate riemann solvers, parameter vectors, and difference schemes. *Journal of Computational Physics*, 43:357–372, 1981.

[13]Y. Liu an M. Vinokur. Upwind algorithms for general thermo-chemical nonequilibrium flows. *AIAA paper No. 1989-0201*, 1989.

[14]J.H. Williamson. Low-storage runge-kutta schemes. *Journal of Computational Physics*, 35(1):48–56, 1980.

[15]Lian Duan and M.P. Martin. An effective procedure for testing the validity of DNS of wall-bounded turbulence including finite-rate reactions. *AIAA Journal*, 47(1):244–251, 2009.

[16]M.P. Martin. DNS of hypersonic turbulent boundary layers. part i: Initialization and comparison with experiments. *Journal of Fluid Mechanics*, 570:347–364, 2007.

[17]S. Xu and M. P. Martin. Assessment of inflow boundary conditions for compressible turbulent boundary layers. *Physics of Fluids*, 16(7):2623–2639, 2004.

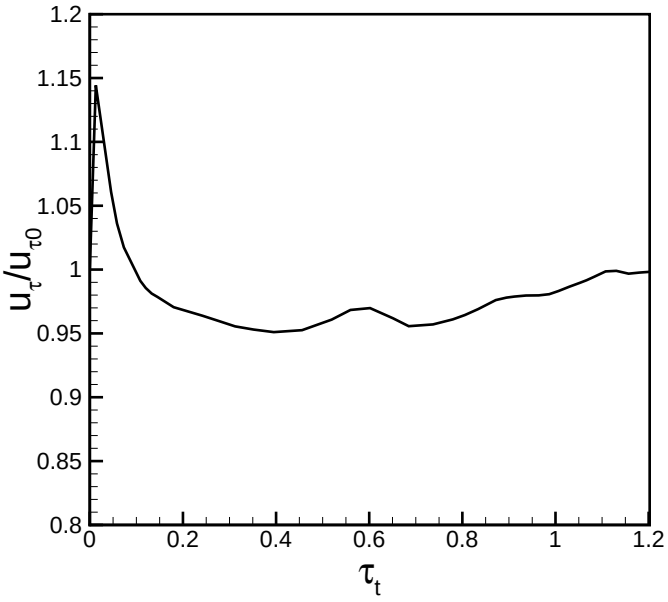

Figure 1. Temporal evolution of the normalized friction velocity

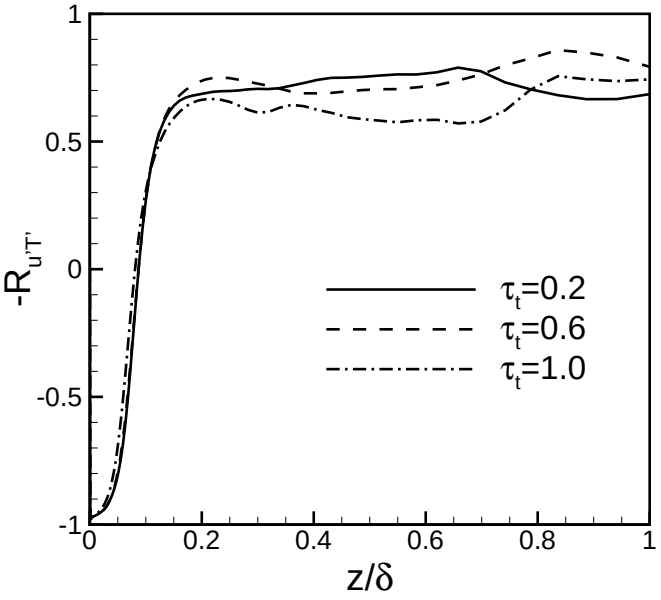

Figure 2. Correlation of stream-wise velocity fluctuation and temperature fluctuation across the boundary layer at different time instances

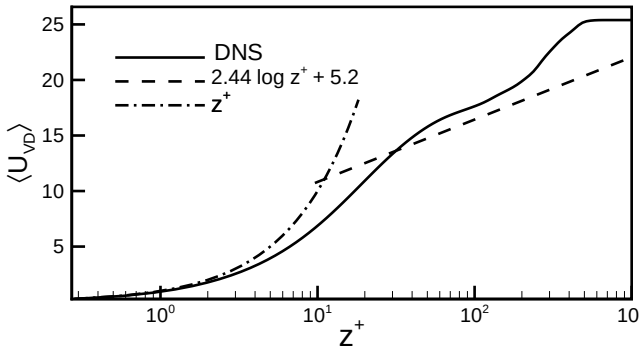

Figure 3. Van Driest transformed velocity profile

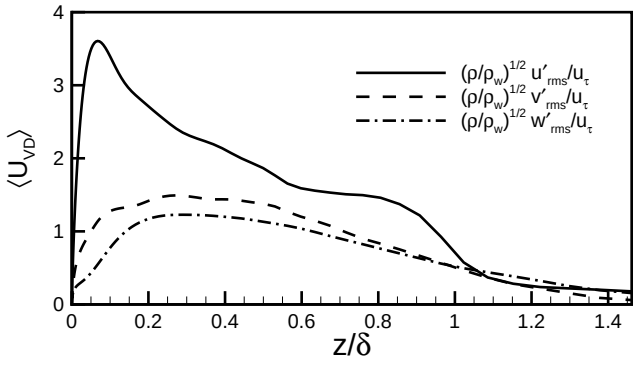

Figure 4. Morkovin scaled turbulent intensities